# Vortex line in a neutral finite-temperature superfluid Fermi gas

N. Nygaard
*Electron and Optical Physics Division, National Institute of Standards and Technology, Gaithersburg, Maryland 20899-8410, USA and Chemical Physics Program, University of Maryland, College Park, Maryland 20742, USA*

G. M. Bruun
*Niels Bohr Institute, Blegdamsvej 17, 2100 Copenhagen, Denmark*

B. I. Schneider
*Physics Division, National Science Foundation, Arlington, Virginia 22230, USA*

C. W. Clark
*Electron and Optical Physics Division, National Institute of Standards and Technology, Gaithersburg, Maryland 20899-8410, USA*

D. L. Feder
*Department of Physics and Astronomy, University of Calgary, Calgary, Alberta, Canada T2N 1N4*
(Received 9 December 2003; published 20 May 2004)

The structure of an isolated vortex in a dilute two-component neutral superfluid Fermi gas is studied within the context of self-consistent Bogoliubov–de Gennes theory. Various thermodynamic properties are calculated, and the shift in the critical temperature due to the presence of the vortex is analyzed. The gapless excitations inside the vortex core are studied, and a scheme to detect these states and thus the presence of the vortex is examined. The numerical results are compared with various analytical expressions when appropriate.

DOI: 10.1103/PhysRevA.69.053622 PACS number(s): 03.75.Ss, 05.30.Fk, 67.57.Fg

## I. INTRODUCTION

The achievement of Fermi degeneracy in a confined gas of alkali-metal atoms [1–7] has spurred great interest both theoretically and experimentally in cold atomic gases with Fermi statistics. The atomic interactions are well understood and often may be tailored through the physics of Feshbach resonances by the application of external magnetic fields [8–10]. When the atom-atom interaction is attractive, the ground state of a two-component gas is predicted to be superfluid at low temperatures [11]. Such a superfluid would provide a unique test bed for the study and interpretation of analogous but much more complex systems, such as superfluid $^3$He, unconventional superconductors, and neutron stars.

One important issue facing the cold atom community has been how one would go about actually detecting the presence of superfluidity in these systems. Superfluidity in Bose-Einstein condensates (BEC's) can be inferred either by probing directly the momentum distribution of the cloud, the collective modes (where the spectrum is strongly shifted relative to the normal phase), or by generating quantized vortices (an unambiguous signature of the breakdown of irrotational flow) and simply viewing the associated "holes" in the particle density [12,13]. Likewise, for superfluid Fermi gases, the presence of superfluidity has been shown to give many observable effects on the mode spectrum of the gas [14,15]. For fermions in the weak-coupling limit, the presence of a vortex would be very difficult to image directly by looking at the density profile, as there is very little depletion of the density in the vortex core [16]. However, the quantization of angular momentum which is a striking macroscopic effect of superfluidity can, as for bosons, be measured through the energy shift of the quadrupole modes [17]. We mention that in the limit of strong interactions superfluidity arises due to Bose-Einstein condensation of tightly bound bosonic molecules, and consequently quantum vortices with a pronounced density contrast are possible [18]. In the present paper we focus on the weak-coupling limit.

Experimental techniques currently limit the temperature of trapped Fermi gases to not much less than one-tenth of the Fermi degeneracy temperature $T_F$. The superfluid transition temperature $T_c$ of a conventional uniform Bardeen-Cooper-Schrieffer (BCS) superconductor, however, is typically lower: $T_c/T_F \simeq 0.28e^{-\pi/2k_F|a|} \ll 1$, with $k_F$ the momentum at the Fermi surface, $a$ the $s$-wave scattering length for low-energy two-body collisions, and $k_F|a| \ll 1$ in the weak-coupling approximation where BCS theory is valid. A number of schemes to raise $T_c$ to a value closer to temperatures already accessible with dilute Fermi gases have recently been proposed. One of these, referred to in the literature as "resonance superfluidity," involves tuning the scattering length to an extremely large value at a Feshbach resonance [19,20]; recent experimental results (see, for example, [21–23]) show significant progress using this approach, culminating in the production of a Bose-Einstein condensate of molecules [24–27]. Another proposal involves loading the cold Fermi gas into a three-dimensional optical lattice [28]: if the lattice is made sufficiently deep, the lowest-lying band will flatten to the point where all of the atoms participate in the pairing, as opposed to regular BCS theory, where only a small fraction of particles close to the Fermi surface are available for pair formation. Of course, the lattice depth cannot be so great that coherence across the sample is destroyed, as has been

observed for bosons in optical lattices [29–31]. The inability to experimentally attain very low temperatures in dilute gases is probably not fundamental, however. With an eye on future experiments, it thus seems reasonable to explore the predictions of a weak-coupling theory of Fermi superfluidity.

In the present paper, we examine in detail several properties of the vortex phase of a neutral Fermi liquid confined in a cylindrical box, presenting the solution of the full microscopic theory at finite temperature. An essential difference from similar studies in the superconductivity literature (see, e.g., [32]) is the absence of an arbitrary cutoff in the sums over quasiparticle states. Since the interactions in dilute quantum gases are characterized entirely by parameters, which can be either calculated from *ab initio* theoretical models or measured experimentally, our theory contains no free parameters. The paper is structured as follows: the theoretical framework is briefly discussed in Sec. II, and we present in Sec. III the details of our numerical procedure. Section IV is devoted to the calculation of various thermodynamic quantities of the vortex phase, which are compared with the corresponding quantities in both the normal state and the superfluid with no vortex. Furthermore, we demonstrate that the vortex causes a shift of the superfluid transition temperature. Finally, in Sec. V we propose a way of observing the vortex through "laser probing" of the quasiparticle states trapped inside the vortex core.

## II. THEORETICAL BACKGROUND

We consider a two-component Fermi gas consisting of particles with internal quantum numbers $\sigma=\uparrow,\downarrow$ and mass $m_a$ confined in an external potential $V_{\rm ext}(\mathbf{r})$. For atomic gases at low temperatures and realistic densities, the interactions far from Feshbach resonances are characterized by the low-energy parameter $a$ which is the $s$-wave scattering length appropriate for the scattering between the two specific internal states of the atoms. Therefore, only Fermi particles in different internal states are able to interact. In our calculations, we assume an equal population of the two components $N_\uparrow=N_\downarrow$ so that their densities $n_\sigma$ are equal. The superfluid phase of the gas for $a<0$ can be described within mean-field theory by the Bogoliubov–de Gennes (BdG) equations [33]

$$\begin{bmatrix} \mathcal{H}^{\rm HF}-\mu & \Delta(\mathbf{r}) \\ \Delta^*(\mathbf{r}) & -(\mathcal{H}^{\rm HF}-\mu) \end{bmatrix} \begin{bmatrix} u_\eta(\mathbf{r}) \\ v_\eta(\mathbf{r}) \end{bmatrix} = E_\eta \begin{bmatrix} u_\eta(\mathbf{r}) \\ v_\eta(\mathbf{r}) \end{bmatrix}. \quad (1)$$

Here $\mathcal{H}^{\rm HF}=(-\hbar^2/2m_a)\nabla^2+V_{\rm ext}(\mathbf{r})+gn_\sigma(\mathbf{r})$ with the low-energy effective coupling constant given by $g=4\pi\hbar^2a/m_a$, and we have taken the interaction to be of zero rage. The particle density and pairing field are defined as $n_\sigma(\mathbf{r})=\langle\psi_\sigma^\dagger(\mathbf{r})\psi_\sigma(\mathbf{r})\rangle$ and $\Delta(\mathbf{r})=-\tilde{g}\langle\psi_\uparrow(\mathbf{r})\psi_\downarrow(\mathbf{r})\rangle$, respectively, where $\psi_\sigma^\dagger(\mathbf{r})$ is the usual fermionic field operator creating a particle in the internal state $\sigma$ at position $\mathbf{r}$. It is important to note that the use of a contact potential gives rise to an unphysical ultraviolet divergence of the pairing field, due to the absence of a high-energy cutoff. We regularize the expression for $\Delta(\mathbf{r})$ using the pseudopotential method [34,35], which introduces a regularized coupling constant $\tilde{g}$.

The Bogoliubov wave functions $u_\eta(\mathbf{r})$ and $v_\eta(\mathbf{r})$ describe quasiparticle excitations with energy $E_\eta>0$. In terms of these the self-consistent density is given by

$$n_\sigma(\mathbf{r})=\sum_\eta\{|u_\eta(\mathbf{r})|^2f(E_\eta)+|v_\eta(\mathbf{r})|^2[1-f(E_\eta)]\}, \quad (2)$$

while the gap equation for the pairing field is

$$\Delta(\mathbf{r})=-\tilde{g}\sum_\eta u_\eta(\mathbf{r})v_\eta^*(\mathbf{r})[1-2f(E_\eta)]. \quad (3)$$

The thermal population of a quasiparticle state with energy $E_\eta$ is determined by the Fermi distribution function $f(E_\eta)=(e^{E_\eta/k_BT}+1)^{-1}$.

### Vortex phase

The superfluid order parameter is a complex number and can thus be written as a real amplitude times a phase

$$\Delta(\mathbf{r})=|\Delta(\mathbf{r})|e^{i\theta(\mathbf{r})}. \quad (4)$$

The superfluid velocity is then given by the spatial variation of the phase of the order parameter

$$\mathbf{v}_s=\frac{\hbar}{2m_a}\nabla\theta(\mathbf{r}), \quad (5)$$

where $2m_a$ is the mass of a Cooper pair. A vortex line corresponds to a rotational superfluid flow with a velocity which decreases with the distance $\rho$ from the axis of rotation as

$$v_s=\frac{\kappa\hbar}{2m_a\rho}. \quad (6)$$

Here $\kappa$ is the strength of the vortex line. This form of the velocity field implies the existence of a core region close to the vortex axis where the kinetic energy is large enough to break the Cooper pairs. Hence the order parameter will be suppressed in the vortex core and will heal to its bulk value over a length scale governed by the coherence length $\xi_{\rm BCS}(T)=\hbar v_F/\pi\Delta_0(T)$, with $v_F=\hbar k_F/m_a$ the Fermi velocity and $\Delta_0(T)$ the temperature-dependent value of the bulk gap away from the vortex core [36].

Due to the single valuedness of the order parameter, the phase $\theta$ must return to the same value modulo $2\pi$ when going around the vortex line. Hence the circulation $\oint\mathbf{v}_s\cdot d\ell$ is restricted to integer multiples of $h/2m_a$. In the present work we will concentrate on vortices of unit circulation $\oint\mathbf{v}_s\cdot d\ell=h/2m_a$.

In summary, a vortex line represents a topological defect in the superfluid order parameter, around which the superfluid velocity field $\mathbf{v}_s$ is tangential. The quantization of the circulation represents one of the hallmarks of a superfluid, and therefore the production and subsequent detection of quantized vortices in an ultracold atomic Fermi gas would be a clear signature for superfluidity in the system.

## III. COMPUTATIONAL METHODS

For a gas confined in a cylinder of radius $R$ and length $L$ it is natural to work in cylindrical coordinates $(\rho,z,\varphi)$, where

$\rho$ measures the perpendicular distance from the symmetry axis, $z$ is the axial coordinate, and $\varphi$ is the azimuthal angle around $\hat{z}$. In this coordinate system the order parameter can be written as $\Delta(\mathbf{r})=|\Delta(\rho,z)|\exp(-i\kappa\varphi)$, with $\kappa=0$ corresponding a phase with no vortex and $\kappa=1$ for a singly quantized vortex along the axis of symmetry. The mean-field density is rotationally invariant: $n_\sigma(\mathbf{r})=n_\sigma(\rho,z)$.

Assuming free motion along the cylinder axis and imposing periodic boundary conditions at $z=\pm L/2$, we write, for the quasiparticle modes,

$$u_\eta(\mathbf{r}) = u_{nmk_z}(\rho)\,\frac{e^{im\varphi}}{\sqrt{2\pi}}\,\frac{e^{ik_z z}}{\sqrt{L}},$$

$$v_\eta(\mathbf{r}) = v_{nmk_z}(\rho)\,\frac{e^{i(m+\kappa)\varphi}}{\sqrt{2\pi}}\,\frac{e^{ik_z z}}{\sqrt{L}}. \tag{7}$$

The allowed values of the angular momentum quantum number are $\{m=0,\pm1,\pm2,\ldots\}$ and $k_z=2\pi\ell/L$, with $\{\ell=0,\pm1,\pm2,\ldots\}$. The radial functions $(u_{nmk_z},v_{nmk_z})$ are taken to be real. With these definitions the BdG equations (1) become

$$\begin{bmatrix} H_m & \Delta(\rho) \\ \Delta^*(\rho) & -H_{m+\kappa} \end{bmatrix}\begin{bmatrix} u_{nmk_z}(\rho) \\ v_{nmk_z}(\rho) \end{bmatrix} = E_{nmk_z}\begin{bmatrix} u_{nmk_z}(\rho) \\ v_{nmk_z}(\rho) \end{bmatrix}, \tag{8}$$

where

$$H_m = \frac{\hbar^2}{2m_a}\left[-\frac{1}{\rho}\frac{\partial}{\partial\rho}\rho\frac{\partial}{\partial\rho}+\frac{m^2}{\rho^2}+k_z^2\right]+gn_\sigma(\rho)-\mu. \tag{9}$$

These are the equations we solve self-consistently through an iterative procedure.

By exploiting the symmetry of the BdG equations (1), we can identify a *negative* energy solution with angular momentum $m$ with a *positive* energy solution with angular momentum $-m-\kappa$. We can therefore generate the entire positive energy spectrum by solving Eq. (8) for $m\geqslant 0$ only and using the transformation

$$E_\eta \to -E_\eta,\ \begin{pmatrix} u_\eta \\ v_\eta \end{pmatrix} \to \begin{pmatrix} v_\eta^* \\ -u_\eta^* \end{pmatrix}, \tag{10}$$

to find the eigenstates with $m<0$.

### Discrete variable representation

The BdG equations in general must be solved numerically. Some of the effects of the vortex that we are interested in, such as the associated shifts in the critical temperature $T_c$ and in the ground-state energy of the gas, are quite hard to calculate numerically as they are very small compared with the corresponding bulk values. For example, to obtain the vortex energy one needs to subtract two large numbers (the ground-state energy of the gas with and without a vortex) to get a small number. This requires a very accurate numerical scheme to solve the BdG equations. Such a scheme is provided by the discrete variable representation (DVR) which recently enabled the microscopic calculation of the vortex energy [16]. DVR's are representations on a basis of functions localized about discrete values of the coordinate. This renders local functions of the coordinate operator approximately diagonal within the DVR basis, making DVR's ideally suited for solving self-consistent problems like the present one, where the matrix elements of the pairing and Hartree fields (local functions) have to be evaluated at each iteration. In addition the representation of the kinetic energy operator is exact. The literature on DVR's is extensive and we shall only convey the central points here. A detailed review of the framework can be found in [37,38].

A DVR exists when there is both a spectral basis of $N$ functions, $\phi_n(x)$, orthonormal over an interval $[a,b]$ with weight function $w(x)$ and a quadrature rule with $N$ points $x_k$ and weights $w_k$:

$$\langle f|g\rangle \equiv \int_a^b dx\, w(x)f(x)g(x) \equiv \sum_{k=1}^{N} w_k f(x_k)g(x_k). \tag{11}$$

This enables a set of coordinate eigenfunctions $\{\psi_i(x), i=1,N\}$ to be defined with the property

$$\psi_i(x_k) = \frac{\delta_{ik}}{\sqrt{w_i}}. \tag{12}$$

We expand the unknown functions $\psi_i(x)$ on the basis $\phi_n$,

$$\psi_i(x) = \sum_{n=1}^{N} \phi_n(x)\langle\phi_n|\psi_i\rangle, \tag{13}$$

and use the quadrature rule (11) and the $\delta$ function property of $\psi_i$ (12) to evaluate the expansion coefficients. The coordinate eigenfunctions are then given by

$$\psi_i(x) = \sum_{n=1}^{N} \sqrt{w_i}\phi_n(x)\phi_n(x_i). \tag{14}$$

This leads to functions $\psi_i(x)$ peaked about $x=x_i$ (see Fig. 1 below). Although the coordinate eigenfunctions are continuous functions of the coordinate, they satisfy the Kronecker $\delta$ property (12) on the quadrature points. Since the $\psi_i(x)$ define a representation in which the coordinate operator is diagonal, the matrix element of any operator $\mathcal{O}(x)$, which is a local function of $x$, is approximately diagonal within the DVR,

$$\langle\psi_i|\mathcal{O}(x)|\psi_j\rangle \simeq \mathcal{O}(x_i)\delta_{ij}, \tag{15}$$

the approximation being due to the use of a truncated basis. Furthermore, since the DVR involves an underlying spectral representation, it is possible to evaluate matrix elements of parts of the Hamiltonian exactly if the $\phi_n(x)$ are chosen to be the eigenfunctions of the corresponding operator (for example, the kinetic energy).

For the problem of quantization in a cylinder the cylindrical Bessel functions form an ideally suited basis for the DVR as suggested in Ref. [39], since the Bessel function of order $m$ is the eigenfuntion for the radial motion of a particle with angular momentum $m\hbar$ in a cylindrical box. They are orthogonal over the range $[0,R]$ with weight function $w(\rho)=\rho$,

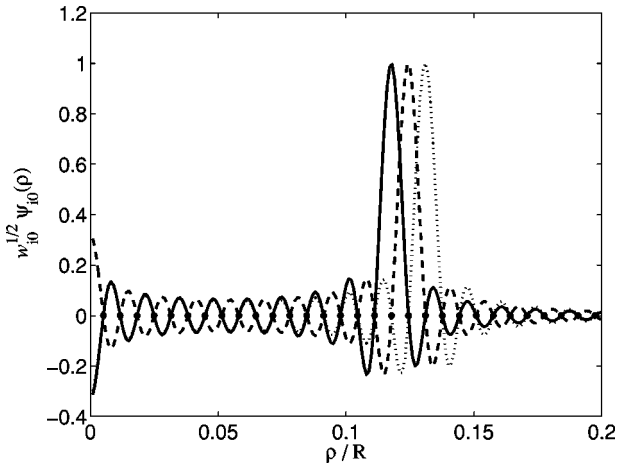


FIG. 1. Examples of coordinate eigenfunctions for a Bessel function DVR based on $J_0$ with $N=150$. For the particular functions plotted $i=18$ (solid line), 19 (dashed line), and 20 (dotted line). The discrete $\delta$ function property of the DVR functions (12) is evident, as $\psi_{i0}(\rho)$ is equal to $w_{i0}^{-1/2}$ at $\rho=\rho_{i0}$, while vanishing on all other DVR points (•).

$$\int_0^R d\rho\, \rho J_m(k_{im}\rho)J_m(k_{jm}\rho) = \frac{\delta_{ij}}{w'_{im}}, \tag{16}$$

provided the momentum grid points are given by $k_{im}=z_{im}/R$, where $\{z_{im}, i=1,\ldots,N\}$ are the zeros of the Bessel function of order $m$, defined through $J_m(z_{im})=0$. This is a consequence of the boundary condition which states that the wave function must vanish at $\rho=R$. The coordinate normalization constant is [40]

$$w'_{im} = \frac{2}{R^2 J_{m+1}^2(k_{im}R)}. \tag{17}$$

Similarly, the Bessel functions are also orthogonal in momentum space,

$$\int_0^{K_m} dk\, kJ_m(k\rho_{im})J_m(k\rho_{jm}) = \frac{\delta_{ij}}{w_{im}}, \tag{18}$$

with the momentum normalization

$$w_{im} = \frac{2}{K_m^2 J_{m+1}^2(K\rho_{im})}. \tag{19}$$

The spatial grid is defined by $\rho_{im}=z_{im}/K_m$. Note that since $k_{Nm}=z_{Nm}/R=K_m$ and $\rho_N=z_{Nm}/K_m=R$, the maximum momentum and the maximum value of $\rho$ are not independent, but are inversely related to each other by the relation $RK_m=z_{Nm}$. It was shown in [39] that a quadrature rule can be associated with these grid points, provided weights are chosen to be $w_{im}$ ($w'_{im}$) for integration over the spatial (momentum) variable. In general there will be one spatial and one momentum grid associated with each value of the azimuthal quantum number $m$.

With the Bessel function quadrature in place we can go ahead and construct a DVR basis. As our orthonormal basis functions we choose

$$\phi_i(\rho) = \sqrt{w'_{im}}J_m(k_{im}\rho), \tag{20}$$

where the $\sqrt{w'_{im}}$ is necessary to ensure that the basis set is orthonormal—i.e., $\langle\phi_k|\phi_l\rangle=\delta_{kl}$. From Eq. (14) we thus have, for the coordinate eigenfunctions,

$$\psi_{im}(\rho) = \sum_n \sqrt{w_{im}}w'_{nm}J_m(k_{nm}\rho)J_m(k_{nm}\rho_{im}). \tag{21}$$

Examples of these functions are plotted in Fig. 1, where the discrete $\delta$ function property (12) is clearly visible. The radial functions $(u_{nmk_z}, v_{nmk_z})$ can be expanded in terms of the coordinate eigenfunctions—i.e., $u_{nmk_z}(\rho)=\Sigma_i\gamma_{im}\psi_{im}(\rho)$. The BdG equations will then be a set of nonlinear equations for the expansion coefficients $\gamma_i$. Due to the properties of the coordinate eigenfunction, the value of the radial function on the grid points is simply $u_{nmk_z}(\rho_{im})=\gamma_{im}/\sqrt{w_{im}}$.

We conclude this section with two important remarks. While the transformation from the spectral basis to the coordinate eigenfunctions is not mathematically unitary due to the truncation of the basis, the numerical procedure is nonetheless well defined, as the transformation can be made unitary in the limit of large $N$ [39]. Second, although it appears that a separate grid is needed for each $m$ value, we have found through numerical experimentation that sufficient accuracy can be achieved using only two grids, one based on $J_0$ for even $m$ and one based on $J_1$ for odd $m$ and treating the centrifugal barrier as an explicit single-particle potential for $m>1$. Since $u_\eta$ and $v_\eta$ for a vortex state correspond to wave functions which differ by one unit of angular momentum, they will be represented on different spatial grids. Fortunately, interpolation is trivial in the DVR method. To interpolate from the $m=0$ to the $m=1$ grid amounts to multiplying the vector of expansion coefficients $\gamma_0$ with the transformation matrix given by $B_{ij}=\psi_{i0}(\rho_{j1})$. The reverse transfomation is $B_{ij}^\dagger=\psi_{i1}(\rho_{j0})$. For the purpose of solving the BdG equations the mean fields are only represented on the odd-$m$ grid.

## IV. THERMODYNAMICS

In this section, we present results for various thermodynamic quantities of the vortex phase obtained by solving the BdG equations numerically as described above. All calculations were done for a fixed $N_\sigma=28\,000$. The radius and length of the box were taken to be $R=28.5$ $\mu$m and $L=11.4$ $\mu$m, respectively. For $^6$Li the scattering length is $-2160a_0$, which gives a bulk value of the transition temperature $T_{c0}=0.01$ $\mu$K and a Fermi temperature of $T_F=0.70$ $\mu$K for the chosen density. With these parameters the coherence length at zero temperature is $\xi_{\mathrm{BCS}}=5.4$ $\mu$m.

In Fig. 2 we plot the free energy $F=\langle\hat{H}\rangle-TS$ as a function of the temperature $T$. The entropy is found as

$$S = -k_B\sum_\eta \{f(E_\eta)\ln f(E_\eta) + [1-f(E_\eta)]\ln[1-f(E_\eta)]\}, \tag{22}$$

since the quasiparticles in our mean-field approach form an ensemble of noninteracting fermions [33]. We have calcu-

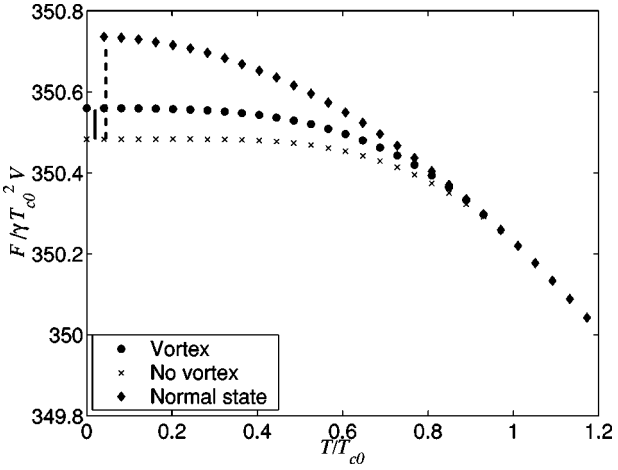


FIG. 2. Plot of the free energy per unit volume of $N_\sigma = 28\,000$ fermions in the normal and superfluid phases with and without a vortex as a function of temperature. The solid and dashed vertical lines represent analytic expressions for the vortex and condensation energies, respectively.

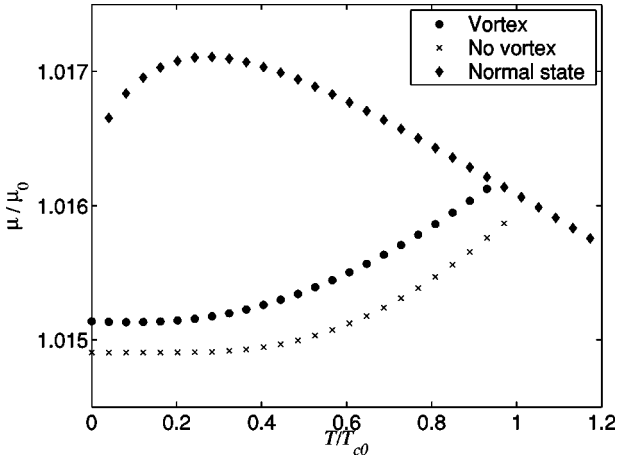


FIG. 3. Chemical potential in the normal and superfluid phases with and without a vortex, as determined by the constraint that $N_\sigma = 28\,000$. We attribute the low-temperature behavior of the normal-phase chemical potential to shell effects due to the finite volume [43]. For the vortex state the transition temperature is shifted downwards.

lated the free energy for the vortex phase, the superfluid phase without a vortex, and for the normal phase. All have been normalized to $\gamma T_{c0}^2$, where $\gamma = 2\pi^2 N(0) k_B^2/3$ and $N(0) = 3n_\sigma/2\epsilon_F$ is the density of states per unit volume (for a single component) at the Fermi energy in the normal phase, $\epsilon_F = \hbar^2 k_F^2/2m_a$ [41]. For $T=0$, the condensation energy density of the superfluid without a vortex with respect to the normal phase is $E_{\rm cond}/V = -N(0)\Delta_0^2/2$, with $\Delta_0 = 8e^{-2}\epsilon_F e^{-\pi/2k_F|a|}$ the bulk value of the superfluid gap. This condensation energy is indicated in the figure, and we see that there is good agreement with the numerical results. Furthermore, the vortex energy per unit axial length for $T=0$ due to the loss of condensation energy in the vortex core and the kinetic energy of the supercurrent around the core is [17]

$$\epsilon_v \approx \frac{\pi\hbar^2 n_\sigma}{2m_a} \ln\left[D\,\frac{R}{\xi_{\rm BCS}(0)}\right]. \tag{23}$$

The constant $D$ was determined numerically in Ref. [16] to be $D \approx 2.5$. This expression for the vortex energy is also indicated in the figure.

As can be seen from Fig. 3, the critical temperature for the vortex phase, $T_{cv}$, is lower than that of the bulk superfluid phase without a vortex, $T_{c0}$. For the specific parameters used, the difference is $1 - T_{cv}/T_{c0} \approx 0.1$. This difference can be understood as follows: The vortex phase becomes unstable with respect to the normal phase when the extent of the vortex core becomes comparable to the radius $R$ of the system. Since the size of the vortex is $\mathcal{O}(\xi_{\rm BCS})$, we can estimate $T_{cv}$ from the condition $\xi_{\rm BCS}(T_{cv}) \sim \mathcal{O}(R)$. Using $\Delta_0(T) \approx 1.7\Delta_0(0)(1 - T/T_{c0})^{1/2}$ [33] for $0 < 1 - T/T_{c0} \ll 1$, this yields

$$\frac{\delta T_c}{T_{c0}} \equiv 1 - \frac{T_{cv}}{T_{c0}} \sim \frac{\xi_{\rm BCS}(0)^2}{R^2}\,\alpha_1, \tag{24}$$

where $\alpha_1$ is a number of order 1. We now test this expression and determine the constant $\alpha_1$ by numerically calculating the shift in the critical temperature, $\delta T_c/T_{c0}$, due to the presence of a vortex for various radii of the system. The result is shown in Fig. 4. We find that we get reasonable agreement with Eq. (24) as $\xi_{\rm BCS}/R \to 0$ with a coefficient $\alpha_1 \approx 2.3$. So one can understand the decrease in $T_c$ due to the presence of the vortex as a finite-size effect which scales as $\xi_{\rm BCS}(0)^2/R^2$.

For a dilute atomic Bose gas the heat capacity in the vicinity of the BEC phase transition has been inferred from a measurement of the energy, which is found from a ballistic expansion of the gas [42]. We therefore expect that this quantity will also be accessible experimentally in the future for dilute Fermi gases. Hence we plot in Fig. 5 the temperature dependence of the heat capacity $c_V = (T/V)\partial S/\partial T$ per unit volume of the system. Again, we show for comparison results both for the system in the normal phase, in the superfluid phase without a vortex, and in the vortex phase. For a two-component gas in the normal phase, we have $c_{V\,\rm normal} = \gamma T$ for $T \to 0$. The heat capacity for the superfluid phase

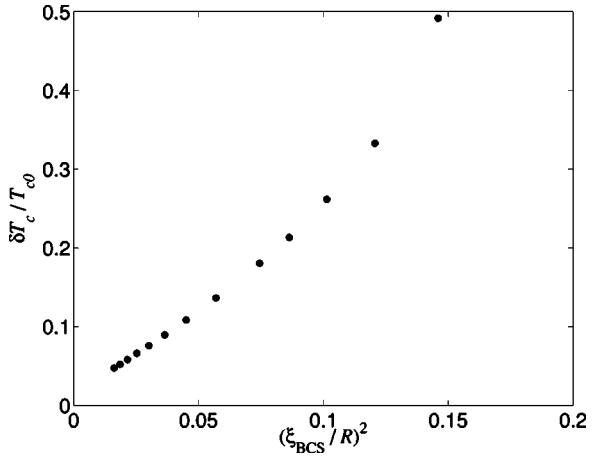


FIG. 4. The shift in the superfluid transition temperature for the vortex state relative to a bulk superfluid with no vortex, as a function of the radius of the confining cylinder at fixed density.

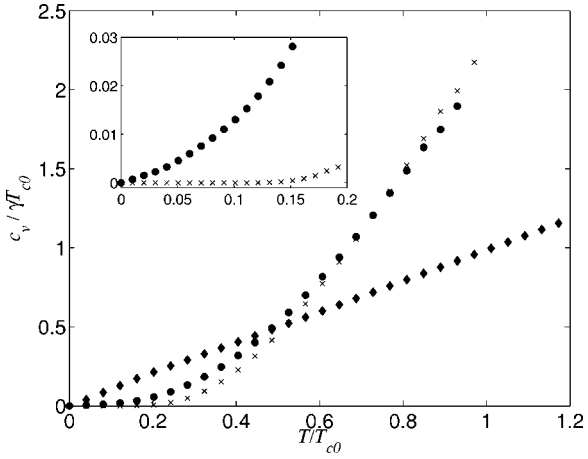


FIG. 5. Plot of the specific heat per unit volume in the normal and superfluid phases with and without a vortex. The inset shows the low-temperature behavior for the vortex state and the superfluid state without a vortex (same symbols as in Figs. 2 and 3).

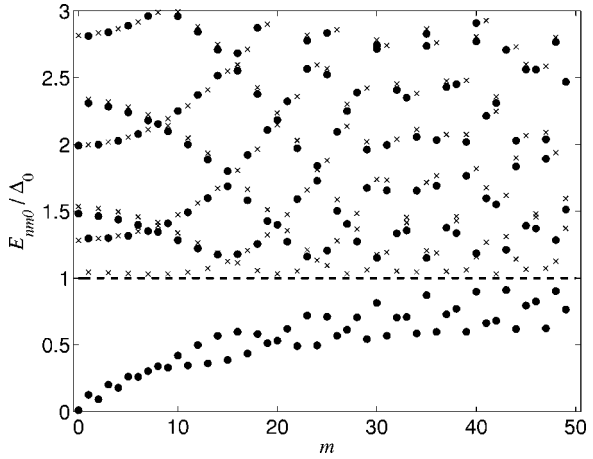


FIG. 6. Energy spectrum for the lowest quasiparticle states in a superfluid with a vortex (•) and the vortex free state (×) at $T=0$. For clarity only the energies of states with $k_z=0$ have been plotted. There are branches of bound states for several values of $k_z$.

without the vortex is exponentially damped by a factor $\exp(-\beta\Delta_0)$ for $T \ll T_c$ due to the gap in the energy spectrum [41]. Figure 5, on the other hand, shows that the heat capacity in the vortex phase, $c_{V\,\mathrm{vortex}}$, depends linearly on $T$ for low temperatures. This linear $T$ dependence is due to the presence of so-called core bound states in the vortex phase. These are single-particle excitations which are spatially localized in the vortex core where the gap is small. The energy of the core states is in general less than the bulk gap energy $\Delta_0$, and they exist only for angular momentum quantum numbers $m \geqslant 0$ [33]. This corresponds to a quasiparticle current around the vortex core in the opposite direction to that of the vortex current. In a detailed analysis it was found that the energy spectrum of the lowest bound core states with $0 \leqslant m \ll k_F\xi_{\mathrm{BCS}}$ for $T=0$ is essentially gapless and given by

$$E_{mk_z} \sim (m+1/2)\,\frac{\Delta_0^2}{\epsilon_F}\frac{h(\theta)}{\sin\theta}, \tag{25}$$

where $k_z=k_F\cos\theta$ and $h(\theta)$ is a function of order unity [44]. In Fig. 6, we plot the lowest quasiparticle energies as a function of $m$ for $k_z=0$ obtained from a numerical solution of Eq. (8). The gapless branch associated with the core states with energies less than $\Delta_0$ is clearly visible. The $T=0$ density of vortex states per unit volume is calculated by integrating Eq. (25) over $k_z$, which yields

$$N_v(\epsilon) = N(0)\alpha_2\,\frac{\xi_{\mathrm{BCS}}^2}{R^2}, \tag{26}$$

for $0 \ll \epsilon \ll \Delta_0$ where $\alpha_2 \sim O(1)$ [45]. Thus, the density of bound core states per unit volume is the same, apart from a factor $\alpha_2$, as that of a cylindrical region of a single-component gas in the normal phase with radius $\xi_{\mathrm{BCS}}$ and length $L$. From this we conclude that the low-$T$ heat capacity per unit volume of the gas in vortex phase $c_{V\,\mathrm{vortex}}$ associated with the core states is

$$c_{V\,\mathrm{vortex}} \sim c_{V\,\mathrm{normal}}\alpha_2\,\frac{\xi_{\mathrm{BCS}}^2}{R^2}, \tag{27}$$

explaining the linear $T$ dependence of $c_{V\,\mathrm{vortex}}$ observed in Fig. 5. A fit to the numerical data yields $\alpha_2 \approx 2$. We remark that a linear contribution to the heat capacity has been observed for a superconductor in the mixed state [46].

## V. LASER PROBING OF THE VORTEX PHASE

Vortices are now routinely created in dilute BEC's where they can be detected by direct imaging of the cores, in which the density is significantly suppressed. Unfortunately, such a procedure would be very difficult to implement successfully for a dilute superfluid Fermi gas, where there is no significant depletion of density in the vortex core [16]. One way to observe the vortex is to measure the shift in the quadrupole mode frequencies which is directly proportional to the angular momentum per particle $\hbar/2$ associated with the supercurrent around the vortex core [17].

In the present section, we investigate the feasibility of detecting the bound quasiparticle states in the vortex core through a recently proposed laser probing scheme [47,48]. The laser probing scheme is similar to scanning tunneling microscopy (STM) on a superconductor in that it relies on induced tunneling between a superfluid and a normal phase [49,50]. Whereas a STM probe uses a bias voltage to transfer population across a superconducting-normal interface existing between the normal microscope tip and the superconducting substrate, the laser probe instead creates an effective interface by coupling different internal states of the atoms by laser fields. Specifically, a spin state $|\uparrow\rangle$, which is Cooper paired with the state $|\downarrow\rangle$, is coupled via a laser field to a third state $|e\rangle$ that has been chosen such that it does not participate in the pairing (either it does not have strong attractive interactions with the two other states or the disparity in chemical potentials is too large). Hence, the $|e\rangle$ atoms define the normal part of the interface. If the detuning of the laser from the

atomic transition is $\delta=\omega_A-\omega_L$, where $\omega_L$ is the laser frequency and $\omega_A$ the frequency splitting between the level $|\uparrow\rangle$ and $|e\rangle$, the rate of change in the population of the $|e\rangle$ state (tunneling current) $I=-\langle\dot{\hat{N}}_e\rangle$ is [48]

$$I(\delta)=-\frac{2\pi}{\hbar}\sum_{\eta,n}\left|\int d^3r\,\Omega(\mathbf{r})u_\eta(\mathbf{r})\Phi_n^*(\mathbf{r})\right|^2\times[f(E_\eta)-f(\xi_n)]\delta(E_\eta-\xi_n-\tilde{\delta})+\left|\int d^3r\,\Omega(\mathbf{r})v_\eta^*(\mathbf{r})\Phi_n^*(\mathbf{r})\right|^2\times[1-f(E_\eta)-f(\xi_n)]\times\delta(E_\eta+\xi_n+\tilde{\delta}). \quad (28)$$

Here $\tilde{\delta}=\mu_e-\mu+\delta\equiv\Delta\mu+\delta$ is the effective detuning, $\mu_e$ the chemical potential of the $|e\rangle$ atoms, and $\Phi_n$ their single-particle wave functions with energy $\xi_n$; $f(x)=[\exp(\beta x)+1]^{-1}$ is the Fermi function and $\Omega(\mathbf{r})$ the Rabi frequency. In the present analysis, we assume for simplicity that the $|e\rangle$ atoms are noninteracting such that their wave functions $\Phi_n$ are the eigenstates of the confining cylindrical box (the coupling strength between the $|e\rangle$ atoms and the particles in the Cooper-paired states could potentially be controlled via a Feshbach resonance, but in any case we anticipate that including the effect of interactions on $\Phi_n$ will not qualitatively change our conclusions). We consider the case of a constant laser profile $\Omega(\mathbf{r})=\Omega$. This gives the selection rule $\mathbf{k}_\uparrow=\mathbf{k}_e$ where $\mathbf{k}_\uparrow$ is the momentum of an $|\uparrow\rangle$ atom coupled by the laser beam to an $|e\rangle$ atom with momentum $\mathbf{k}_e$.

Let us now consider how the laser probing method can be used to probe the presence of the core states. We examine two opposite cases of interest: the case when there are initially no $|e\rangle$ atoms present ($N_e=0$) and the case where there initially are an equal number of $|\uparrow\rangle$ and $|e\rangle$ atoms present ($N_\uparrow=N_e$).

From Eq. (28) it is straightforward to show that for the total current we have $\int d\delta I(\delta)\propto N_e-N_\uparrow$. That is, the net current from the $|e\rangle$ atoms to the $|\uparrow\rangle$ atoms is proportional to the difference of initial populations between the two hyperfine states. Likewise, the total current from the core states trapped inside the vortex is clearly proportional to the total number of core states, $N_{\mathrm{cs}}$. Thus, when there initially are no $|e\rangle$ atoms present ($N_e=0$) the spectral weight of the current due the core states as compared to the total current observed scales as $N_{\mathrm{cs}}/N_\uparrow$. Using $N_{\mathrm{cs}}\sim N_v\Delta_0\pi R^2L$ with $N_v$ given by Eq. (26), one obtains that the current from the core states divided by the total current scales as $\Delta_0\epsilon_F^{-1}\xi_{\mathrm{BCS}}^2R^{-2}\ll 1$. Thus, the signal from the core states is completely overwhelmed by the bulk signal coming from the current out of the whole Fermi sea of $|\uparrow\rangle$ atoms. We therefore conclude that it is most likely not possible to probe the core states starting with initially no $|e\rangle$ present. This conclusion is supported by numerical simulations.

Let us therefore consider the case when there initially are an equal number of $|\uparrow\rangle$ and $|e\rangle$ atoms present ($N_\uparrow=N_e$). In that way, the bulk signal of transitions of $|\uparrow\rangle$ atoms deep within the Fermi sea is Pauli blocked due to the presence of the $|e\rangle$ atoms, since we have the selection rule $\mathbf{k}_\uparrow=\mathbf{k}_e$. One can then show from Eq. (28) that the total signal scales as

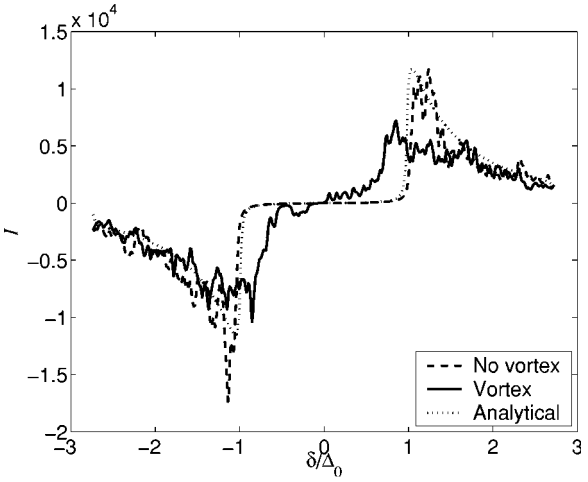


FIG. 7. The tunneling current as a function of detuning (in units of the bulk value of the gap) for tunneling into a filled state from both a vortex state and a superfluid without a vortex. For comparison Eq. (29) is also plotted. The profiles have been shifted to compensate for the Hartree mean-field shift $gn_\sigma$ of the energies of the $|\uparrow\rangle$ atoms. If the $|\uparrow\rangle$ atoms are in the normal state, no current flows due to Pauli blocking.

$\int d\delta|I(\delta)|\propto N_\uparrow\Delta_0/\epsilon_F$; i.e., the current is proportional to the total number of Cooper pairs. Thus, the bulk signal is suppressed by a factor $\Delta_0/\epsilon_F$ compared to the case when there are no $|e\rangle$ atoms present simply due to the Fermi blocking effect. The current due to the vortex core states should therefore be easier to observe as it is not overwhelmed by a huge background signal. In Fig. 7 we plot the $T=0$ laser probing current $I(\delta)$ for the case when $N_e=N_\uparrow$. The effect of the Hartree field $gn_\sigma$ is primarily to shift the entire profile to lower detunings $\delta$ since it shifts the energies of the $|\uparrow\rangle$ atoms by the amount $gn_\sigma$, whereas the $|e\rangle$ atoms are assumed noninteracting. In the plot we have explicitly eliminated this overall shift for reasons of clarity. The neglect of the mean-field potential for the $|e\rangle$ atoms causes an asymmetry of the current profile. We plot the current both when there is no vortex, and when there is a vortex. In the case of no vortex, the current given by Eq. (28) at zero temperature can for a bulk system be shown to be

$$I=\pm\frac{\pi\Omega^2}{\hbar}\rho(\delta)\Theta(\delta^2-\Delta_0^2)\frac{\Delta_0^2}{\delta^2}, \quad (29)$$

where $\pm$ corresponds to $\delta>0$ and $\delta<0$, respectively, and $\rho(\delta)=Vm^{3/2}(\Delta_0^2/\delta-\delta+2\mu)^{1/2}/2\pi^2\hbar^3$ [47,48]. From Eq. (29) it follows that there is no current for detunings with $-\Delta_0<\delta<\Delta_0$. This can be interpreted as the laser signal having to provide a minimum energy $\Delta_0$ to break a Cooper pair and generate a current. Equation (29) is also shown in Fig. 7,

and we see good agreement with the numerical result when there is no vortex present. Note that since the numerical calculations use a Lorentzian of width $\Gamma=0.01\Delta_0$ instead of $\delta(x)$ functions in Eq. (28), we have convoluted Eq. (29) accordingly. We see that the signal when there is a vortex present is markedly different from the case with no vortex. In particular, there is a significant current for $|\delta|<\Delta_0$. This current is directly due to the presence of the core states which have a pairing energy less than $\Delta_0$. The signal from the vortex phase is finite for $\delta\sim 0$, reflecting the fact that the energy spectrum of the core states approximately given by Eq. (25) is essentially gapless. Thus, the existence of core states bound in the vortex is reflected in the current profile $I(\delta)$.

## VI. CONCLUSIONS

We have studied the properties of a single vortex in a neutral superfluid with Fermi statistics using a microscopic weak-coupling theory. The effect of the vortex on the free energy and the heat capacity of the system was examined, and we provided various analytical expressions which agree well with the numerical results. The vortex gives rise to the presence of core states bound in the vortex core. We examined the spectrum of these states and also suggested a way to experimentally detect them. Apart from being of interest theoretically, it is likely that our results will have experimental relevance in the near future due to the recent impressive experimental progress within the field of atomic Fermi gases.


[1] B. DeMarco and D. S. Jin, Science **285**, 1703 (1999).
[2] A. W. Truscott, K. E. Strecker, W. I. McAlexander, G. B. Partridge, and R. G. Hulet, Science **291**, 2570 (2001).
[3] F. Schreck, G. Ferrari, K. L. Corwin, J. Cubizolles, L. Khaykovich, M. O. Mewes, and C. Salomon, Phys. Rev. A **64**, 011402(R) (2001).
[4] S. R. Granade, M. E. Gehm, K. M. O'Hara, and J. E. Thomas, Phys. Rev. Lett. **88**, 120405 (2002).
[5] Z. Hadzibabic, C. A. Stan, K. Dieckmann, S. Gupta, M. W. Zwierlein, A. Görlitz, and W. Ketterle, Phys. Rev. Lett. **88**, 160401 (2002).
[6] G. Roati, F. Riboli, G. Modugno, and M. Inguscio, Phys. Rev. Lett. **89**, 150403 (2002).
[7] S. Jochim, M. Bartenstein, G. Hendl, J. H. Denschlag, R. Grimm, A. Mosk, and M. Weidemüller, Phys. Rev. Lett. **89**, 273202 (2002).
[8] H. Feshbach, Ann. Phys. (N.Y.) **5**, 357 (1958).
[9] H. Feshbach, Ann. Phys. (N.Y.) **19**, 287 (1962).
[10] E. Tiesinga, B. J. Verhaar, and H. T. C. Stoof, Phys. Rev. A **47**, 4114 (1993).
[11] H. T. C. Stoof, M. Houbiers, C. A. Sackett, and R. G. Hulet, Phys. Rev. Lett. **76**, 10 (1996).
[12] M. R. Matthews, B. P. Anderson, P. C. Haljan, D. S. Hall, C. E. Wieman, and E. A. Cornell, Phys. Rev. Lett. **83**, 2498 (1999).
[13] K. W. Madison, F. Chevy, W. Wohlleben, and J. Dalibard, Phys. Rev. Lett. **84**, 806 (2000).
[14] M. A. Baranov and D. S. Petrov, Phys. Rev. A **62**, 041601 (2000).
[15] G. M. Bruun and B. R. Mottelson, Phys. Rev. Lett. **87**, 270403 (2001).
[16] N. Nygaard, G. M. Bruun, C. W. Clark, and D. L. Feder, Phys. Rev. Lett. **90**, 210402 (2003).
[17] G. M. Bruun and L. Viverit, Phys. Rev. A **64**, 063606 (2001).
[18] A. Bulgac and Y. Yu, Phys. Rev. Lett. **91**, 190404 (2003).
[19] M. Holland, S. J. J. M. F. Kokkelmans, M. L. Chiofalo, and R. Walser, Phys. Rev. Lett. **87**, 120406 (2001).
[20] E. Timmermans, K. Furuya, P. W. Milonni, and A. K. Kerman, Phys. Lett. A **285**, 228 (2001).
[21] K. M. O'Hara, S. L. Hemmer, M. E. Gehm, S. R. Granade, and J. E. Thomas, Science **298**, 2179 (2002).
[22] T. Bourdel, J. Cubizolles, L. Khaykovich, K. M. F. Magalhães, S. J. J. M. F. Kokkelmans, G. V. Shlyapnikov, and C. Salomon, Phys. Rev. Lett. **91**, 020402 (2003).
[23] K. E. Strecker, G. B. Partridge, and R. G. Hulet, Phys. Rev. Lett. **91**, 080406 (2003).
[24] M. Greiner, C. A. Regal, and D. S. Jin, Nature (London) **426**, 537 (2003).
[25] S. Jochim, M. Bartenstein, A. Altmeyer, G. Hendl, S. Riedl, C. Chin, J. D. Denschlag, and R. Grimm, Science **302**, 2101 (2003).
[26] M. W. Zwierlein, C. A. Stan, C. H. Schunck, S. M. F. Raupach, S. Gupta, Z. Hadzibabic, and W. Ketterle, Phys. Rev. Lett. **91**, 250401 (2003).
[27] C. A. Regal, M. Greiner, and D. S. Jin, Phys. Rev. Lett. **92**, 040403 (2004).
[28] W. Hofstetter, J. I. Cirac, P. Zoller, E. Demler, and M. D. Lukin, Phys. Rev. Lett. **89**, 220407 (2002).
[29] B. P. Anderson and M. A. Kasevich, Science **282**, 1686 (1998).
[30] C. Orzel, A. K. Tuchman, M. L. Fenselau, M. Yasuda, and M. A. Kasevich, Science **291**, 2386 (2001).
[31] M. Greiner, O. Mandel, T. Esslinger, T. W. Hänsch, and I. Bloch, Nature (London) **415**, 39 (2002).
[32] François Gygi and Michael Schlüter, Phys. Rev. B **43**, 7609 (1991).
[33] P. G. de Gennes, *Superconductivity of Metals and Alloys* (Addison-Wesley, New York, 1989).
[34] G. Bruun, Y. Castin, R. Dum, and K. Burnett, Eur. Phys. J. D **7**, 433 (1999).
[35] A. Bulgac and Y. Yu, Phys. Rev. Lett. **88**, 042504 (2002).
[36] We can estimate the radius of the cylinder in which interior superfluidity will be suppressed by equating the kinetic energy $\frac{1}{2}m\mathbf{v}_s^2$ with the condensation energy per particle, $3\Delta_0^2/8\mu$. This gives just $\sim\xi_{\mathrm{BCS}}$.
[37] D. Baye and P.-H. Heenen, J. Phys. A **19**, 2041 (1986).
[38] J. C. Light and T. Carrington, Jr., Adv. Chem. Phys. **114**, 263 (2000).
[39] D. Lemoine, J. Chem. Phys. **101**, 1 (1994).
[40] G. B. Arfken and H. J. Weber, *Mathematical Methods for Physicists*, 4th ed. (Academic Press, San Diego, 1995).
[41] A. L. Fetter and J. D. Walecka, *Quantum Theory of Many-Particle Systems* (McGraw-Hill, New York, 1971).

[42] J. R. Ensher, D. S. Jin, M. R. Matthews, C. E. Wieman, and E. A. Cornell, Phys. Rev. Lett. **77**, 4984 (1996).
[43] J. Schneider and H. Wallis, Phys. Rev. A **57**, 1253 (1998).
[44] C. Caroli, P. G. D. Gennes, and J. Matricon, Phys. Lett. **9**, 307 (1964).
[45] A. L. Fetter, in *Superconductivity*, edited by R. D. Parks (Marcel Dekker, New York, 1969), Vol. I.
[46] P. H. Keesom and R. Radebaugh, Phys. Rev. Lett. **13**, 685 (1964).
[47] P. Törma and P. Zoller, Phys. Rev. Lett. **85**, 487 (2000).
[48] G. M. Bruun, P. Törma, M. Rodriguez, and P. Zoller, Phys. Rev. A **64**, 033609 (2001).
[49] H. F. Hess, R. B. Robinson, R. C. Dynes, J. M. Valles, Jr., and J. V. Waszczak, Phys. Rev. Lett. **62**, 214 (1989).
[50] H. F. Hess, R. B. Robinson, and J. V. Waszczak, Phys. Rev. Lett. **64**, 2711 (1990).